

Article

Sensitivity and Resolution of Controlled-Source Electromagnetic Method for Gas Hydrate Stable Zone

Zhenwei Guo ^{1,2,3} , Yunxi Yuan ^{1,2,3}, Mengyuan Jiang ³, Jianxin Liu ^{1,2,3} , Xianying Wang ⁴ 
and Bochen Wang ^{1,2,3,*}

¹ Key Laboratory of Metallogenic Prediction of Nonferrous Metals and Geological Environment Monitoring, Central South University, Ministry of Education, Changsha 410083, China; guozhenwei@csu.edu.cn (Z.G.); yuanyunxi@csu.edu.cn (Y.Y.); ljx6666@126.com (J.L.)

² Hunan Key Laboratory of Nonferrous Resources and Geological Hazard Exploration, Changsha 410083, China

³ Department of Applied Geophysics, School of Geosciences and Info-Physics, Central South University, Changsha 410083, China; 8211191324@csu.edu.cn

⁴ Guangzhou Marine Geological Survey, Guangzhou 510075, China; xianyingwang@ucas.ac.cn

* Correspondence: bochenwang29@csu.edu.cn; Tel.: +86-18247218058

Abstract: Natural gas hydrate is one of the most important clean energies and part of carbon cycle, due to the least carbon content. Natural gas hydrates depend on high pressure and low temperatures, located under seabed or permafrost. Small changes in temperature and pressure may lead gas hydrates to separate into water and gas, commonly as methane. As a powerful greenhouse gas, methane is much stronger than carbon dioxide. Therefore, it is necessary to detect the gas hydrates stable zone (GHSZ) before the methane gas escapes from GHSZ. Marine controlled source electromagnetic method (CSEM) is a useful tool to detect gas hydrate in offshore. The results from 3D CSEM method are a resistivity cube to describe the distribution of gas hydrates. In order to study the detectability of CSEM method, we simulate the sensitivity and resolution of marine CSEM synthetic data. By using the sensitivity and resolution, a simple statement may be quickly judged on the existence and occurrence range of the natural gas hydrate. In this paper, we compare the resolution of marine CSEM method with various transverse resistance. This information may help researchers find out whether the GHSZ exists or not.

Keywords: gas hydrate; CSEM; resolution; sensitivity



Citation: Guo, Z.; Yuan, Y.; Jiang, M.; Liu, J.; Wang, X.; Wang, B. Sensitivity and Resolution of Controlled-Source Electromagnetic Method for Gas Hydrate Stable Zone. *Energies* **2021**, *14*, 8318. <https://doi.org/10.3390/en14248318>

Academic Editors: Eugen Rusu, Kostas Belibassakis, George Lavidas and Bashir A. Arima

Received: 7 October 2021

Accepted: 1 December 2021

Published: 10 December 2021

Publisher's Note: MDPI stays neutral with regard to jurisdictional claims in published maps and institutional affiliations.



Copyright: © 2021 by the authors. Licensee MDPI, Basel, Switzerland. This article is an open access article distributed under the terms and conditions of the Creative Commons Attribution (CC BY) license (<https://creativecommons.org/licenses/by/4.0/>).

1. Introduction

Energy issues are closely related to the survival and development of mankind. Due to the reduction of conventional energy sources, it is of great significance to find a new energy source to replace all known petroleum gas resources. Gas hydrate was originally discovered in the Arctic permafrost. It is a solid like ice that exists in the seabed sediments on the margins of the continent. The main components of natural gas hydrate are methane (CH₄) and water. Methane gas is a clean and green energy. Its resources are particularly huge. It is known that the global abundance of methane frozen in hydrate exceeds all other existing sources [1]. Due to the wide distribution of gas hydrate, abundant resources and clean combustion, scientists call combustible ice “the strategic commanding heights of global energy development in the future”. Many countries that do not have conventional hydrocarbon resources and energy importers, such as Japan, China, India, and the United States, regard combustible ice as a potential energy resource [2–4].

Marine CSEM method is one of early hydrocarbon reservoir exploration tools in offshore environment [5–8]. In geophysical prospecting, especially marine geophysical prospecting, marine CSEM method plays a pivotal role. CSEM method is a kind of geophysical method that is very sensitive to resistivity anomaly because the resistivity of

the background sedimentary layer is lower than that of the sedimentary layer containing natural gas hydrate. Therefore, the CSEM method has always been an important supplementary method to the seismic method. In the early research, marine CSEM method was used to detect mid-ocean ridges [9,10]. Besides, it was gradually tested in the natural gas hydrates deposits exploration [11]. Some applications of the marine CSEM method successfully improved the rate of drilling [12,13]. For example, Schwalenberg et al., applied marine CSEM method to the exploration of natural gas hydrate in the offshore waters of New Zealand [14,15]. The results obtained from simultaneous 1D and 2D inversion of the marine CSEM data are very consistent with those of seismic results, suggesting that the ocean CSEM method is suitable for gas hydrate exploration. China University of Geosciences used marine CSEM method to conduct hydrate detection experiments in Qiongdongnan waters [16]. Tharimela et al., applied 3D CSEM imaging to the exploration of natural gas hydrates in the Pelotas Basin offshore Brazil [17]. Weitemeyer conducted gas hydrate exploration in the offshore Oregon. The success of this exploration proved that marine CSEM method is feasible in gas hydrate exploration [18].

In order to test the effects of CSEM method on natural gas hydrates exploration, modeling and inversion are the economic way to simulate the electromagnetic data. Moreover, the difference between the data of target response and the background response from the CSEM modeling is too small to be captured. Compared with forward modeling, inversion has high reliability. However, inversion is computationally expensive. Therefore, it is of great significance to find a more reliable and fast method to quickly determine whether gas hydrate exists and roughly delineate the spatial extent of gas hydrate.

In marine CSEM method, sensitivity and resolution are both important parameters for evaluating the detection capability.

The conventional sensitivity calculation method usually performs the calculation of the sensitivity matrix. The sensitivity matrix can be calculated mainly by perturbation method [19], sensitivity equation [20,21] and adjoint equation [22]. However, the solution of the sensitivity matrix requires a huge amount of memory due to its huge amount of calculation and requires huge time. McGillivray and Oldenburg explored how to find the existing options of the inversion problem and calculate the sensitivity efficiently. The finite difference approximation was used to calculate the model parameters, so as to calculate the sensitivity or the quantity related to the sensitivity solution, and the first-order sensitivity calculation was extended to the calculation of the direction, the higher order and the sensitivity to the objective function [23]. A simple derivation was made for the solution of sensitivity in electromagnetic inversion, and the adjoint operator was not used in the derivation process. Although there was no Green's function method practical, it could save more time and cost due to its simplicity [24]. Spies and Habashy proposed a sensitivity calculation based on the use of the reciprocity theorem, which greatly improved the efficiency of sensitivity calculation [25]. Gribenko and Zhdanov used the quasi-analytical approximation method of variable background (QAVB) for sensitivity calculations, which greatly simplified all calculations. This method was more efficient for ocean CSEM method with multiple sources and receivers [26]. Based on the principle of reciprocity, the comprehensive sensitivity method of multiple transmitters and receivers was explored, which proved the importance of sensitivity for marine CSEM method [27]. This method is more efficient for ocean CSEM method with multiple sources and receivers. Mittet and Morten proposed a simplified method for calculating sensitivity, which does not involve the calculation of sensitivity matrix and greatly simplifies the solution of sensitivity [28].

Among the geophysical exploration methods, the resolution of marine CSEM method is relatively low. Scholl and Edwards compared the resolution of the vertical electric dipole TX in the borehole and the standard seafloor array [29]. They found that, if both arrays are extended to a proper offset, the array from downhole to the seafloor seems to have higher horizontal resolution but poor one in the vertical direction, and the resolution can be increased by using different TX positions. Gao et al., proposed a method for

evaluating the resolution and uncertainty of images generated by large-scale nonlinear EM inversion schemes and provided examples demonstrating the calculation efficiency [30]. Morten et al., proposed a regularization method to enhance the resolution in anisotropic 3D inversion of marine CSEM data [31]. To understand the sensitivity and resolution of marine CSEM method for detecting electrical anisotropy in reservoirs, Brown et al., conducted a series of studies and found that when the target horizontal resistivity is higher than the background, the resolution will be slightly better [32]. And usually for 3D inversion, the vertical resistivity of the reservoir is better resolved than the horizontal resistivity. Moghadas et al., studied the impact of seabed topography and seabed structure on marine CSEM data and resolution through numerical simulation methods in shallow and deep-water environments [33]. Sasaki proposed an anisotropic 3D inversion algorithm for marine CSEM data by applying the same vertical and horizontal resistivity, a resistive reservoir can be better distinguished [34]. Blatter et al., performed a joint inversion of marine CSEM and MT data collected from the sea in New Jersey, USA, and obtained better resolution results [35]. Ren and Kalscheuer provided an overview of the model uncertainty and resolution analysis of 2D and 3D electromagnetic data [36].

In this paper, we focus on the sensitivity and resolution of marine CSEM method research, which are important to natural gas hydrate. Since the resistivity of natural gas hydrate varies with water saturation, the resistivity ranges from a few to hundreds of ohms [37]. Therefore, how to improve the resolution and sensitivity of the inversion has become a very challenging subject. A method for determining whether there is gas hydrate in the target area and delineating the approximate spatial extent of gas hydrate by calculating sensitivity instead of inverting marine CSEM data is in urgent need. In this study, we test different resistivity values of the anomalous bodies with a fixed the water depth, and change the water depths with a given resistivity of the anomalies to explore the resolution of marine CSEM method. Therefore, the calculation time and calculation cost can be greatly reduced.

2. Methods

In this study, we employ MARE2DEM to forward and inverse the model [28]. The forward analysis is based on the adaptive finite element method and the inversion relies on the Occam inversion. The finite element method is a partial differential equation solving method that converts partial differential equations into algebraic equations by dividing the solution area into simple geometric unit grids and approximating the basic functions in each grid. The cell size and basis function will affect the accuracy of the solution [38]. The adaptive finite element method, proposed by Babuška et al. [29,30], can automatically adjust the grid elements and basic functions during the calculating process and finally yields an optimal grid size. The adaptive finite element method has the advantages of high accuracy, high efficiency, high reliability, and strong adaptability [38].

Occam inversion is a regularized inversion method which is independent of the initial model [30]. This method yields the best solution with the smallest model roughness and smallest misfit between the simulated and observed data. It has good convergence stability. In this article, we invert the data with 3% noise following the work by Mittet and Marten [28].

Mittet and Morten defined the sensitivity of marine CSEM method through derivation as [28].

$$\Psi(r_r|r_s, \omega) = \left| \frac{\Delta E_x(r_r|r_s, \omega)}{\delta E_x(r_r|r_s, \omega)} \right| \quad (1)$$

where $\Psi(r_r|r_s, \omega)$ is the sensitivity (r_r is the location of receiver, r_s is the location of the source, and ω is frequency). $\Delta E_x(r_r|r_s, \omega)$ represents the difference in electromagnetic response between the target field $E_x^A(r_r|r_s, \omega)$ and background field $E_x^B(r_r|r_s, \omega)$:

$$\Delta E_x(r_r|r_s, \omega) = E_x^A(r_r|r_s, \omega) - E_x^B(r_r|r_s, \omega) \quad (2)$$

$\delta E_x(r_r|r_s, \omega)$ represents the uncertainty caused by the position of source and receivers and calibration of the marine CSEM method. Its mathematical definition is given as follows:

$$\delta E_x(r_r|r_s, \omega) = \sqrt{\alpha |E_x^A(r_r|r_s, \omega)|^2 + N^2} \quad (3)$$

where α is the influence factor and N is the white noise.

In order to calculate the uncertainty, we need the information of α and N . Here we take 3% noise level [28]. The white noise N is related to water depth. For other sea depths, we use cubic spline interpolation to obtain white noise [28].

The lateral resistance is a parameter related to the product of resistivity and thickness of the layered model, and does not change when the product of the two remains unchanged. Anomalous transverse resistance (ATR) represents the resistivity contrast accumulated by abnormalities in the area and it depends on the integral of the difference between the resistivity of the reservoir and the resistivity of the sedimentary layer and the thickness of the reservoir [31].

$$ATR = \int \Delta R(z) dz \quad (4)$$

where ΔR is the difference between the resistivity of the reservoir and the resistivity of the sedimentary layer.

The equivalent expression of the discretization of equation (4) can be expressed as:

$$ATR_{inv} = \sum (\Delta R_{CSEM} \times \Delta z) = \int \Delta R_{CSEM}(z) dz \quad (5)$$

where ATR_{inv} is the lateral resistance anomaly of the inversion result, and Δz is the differential thickness of the reservoir. If we calculate the sensitivity at the location of the receivers, the ATR_{inv} will be computed as a pseudo-well to describe the sensitivity of the target well.

3. Results

In order to test the resolution of marine CSEM method, we separately explored the difference between the abnormal body and the surrounding sediments and the buried depth of the abnormal body as variables. In order to measure the minimum lateral resistance to study the electromagnetic resolution, we have constructed seven models with the seawater depth of 1000 m and seawater resistivity of $0.3 \Omega \cdot m$. In the tests, we set the size of the target layer, i.e., a high-resistance anomaly, to be $5000 \text{ m} \times 100 \text{ m}$. The resistivities of the seven models are 102, 52, 22, 12, 10, 6, 5, and $4 \Omega \cdot m$, respectively. The transmitter adopts the frequency of 0.25, 0.5, 0.75, 1, 1.25, 1.5, 2, and 5 Hz, respectively. The transverse resistance (TR) of each model is assigned to be 10000, 5000, 2000, 1000, 800, 400, 300 and $200 \Omega \cdot m^2$, respectively. The details of the seven models are given in Table 1.

Table 1. Model parameters of the marine CSEM method [38].

	Resistivity ($\Omega \cdot m$)	Thickness (m)	Length (m)
Air	10^{13}		
Sea Water	0.3	1000	
Target	102, 52, 22, 12, 10, 6, 5, 4	100	5000
Sediments	2		

The inversion results of the seven models are summarized in Figure 1. It is clear that we can recover the position of the anomaly well when the thickness of the anomaly is 100 m and the resistivity is $6 \Omega \cdot m$. However, the inversion results are not satisfactory when the resistivity decreases to a lower value, e.g., $5 \Omega \cdot m$.

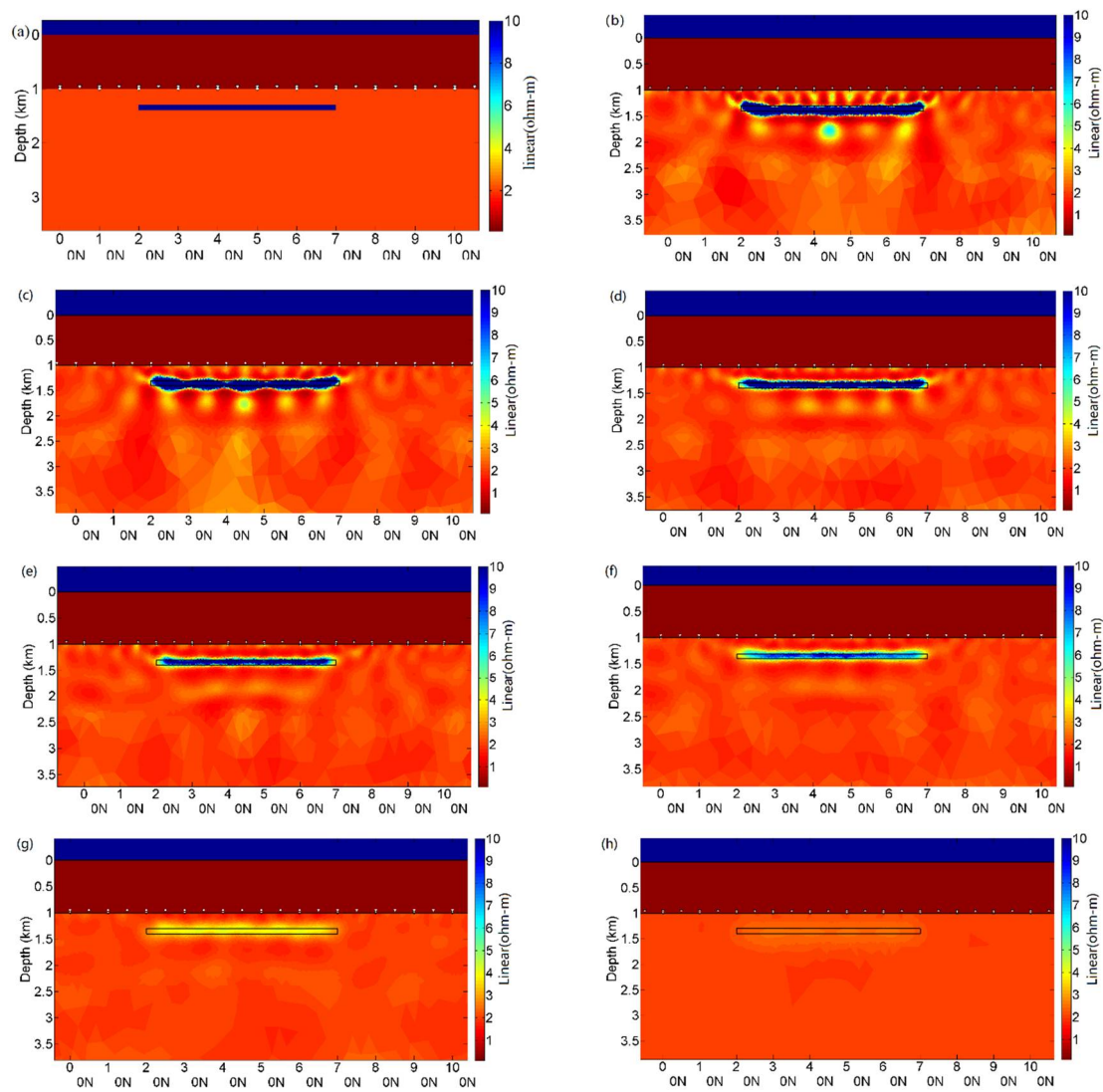


Figure 1. Initial model and inversion results of different values of TR. (Change resistivity of targets) (a) initial model; (b) TR: $10,000 \Omega \cdot \text{m}^2$; (c) TR: $5000 \Omega \cdot \text{m}^2$; (d) TR: $2000 \Omega \cdot \text{m}^2$; (e) TR: $1000 \Omega \cdot \text{m}^2$; (f) TR: $800 \Omega \cdot \text{m}^2$; (g) TR: $400 \Omega \cdot \text{m}^2$; (h) TR: $300 \Omega \cdot \text{m}^2$.

Next, we explored the influence of the depth of the anomaly on the resolution of marine CSEM method. We set the seawater depth to 2500 m. Notice that the seawater resistivity and the size of the anomaly remain unchanged. We then set the resistivity of the anomaly to $6 \Omega \cdot \text{m}$. According to the gas hydrate phase equilibrium curve [39], the maximum burial depth of marine gas hydrate is 3100 m under the condition of the water depth = 2500 m, therefore we set the burial depths of the anomalous bodies to be 200, 400, and 600 m, respectively, below the seabed. The inversion results of these three models are shown below (Figure 2).

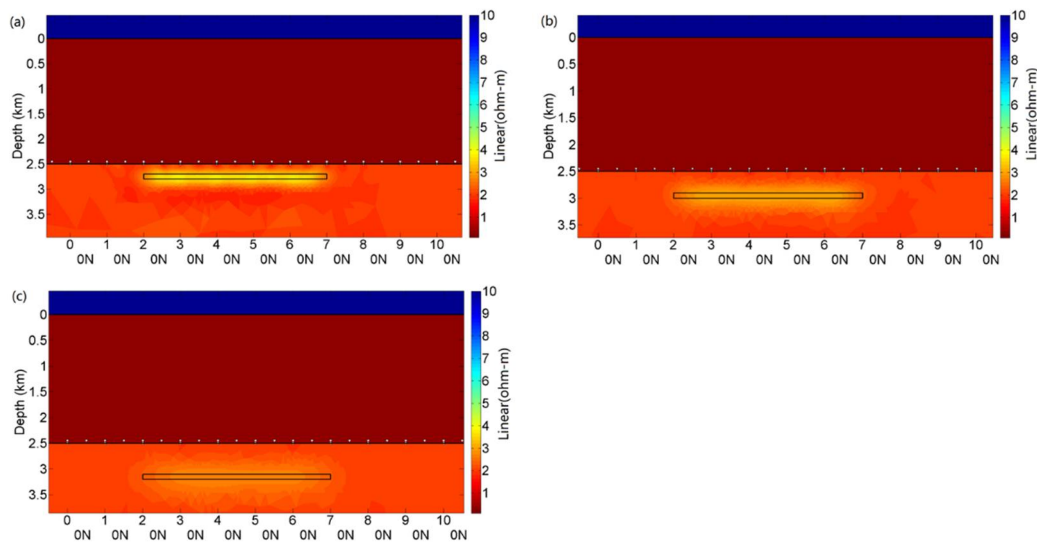


Figure 2. Inversion results of different values of the target depth. (a) Burial depth: 200 m; (b) Burial depth: 400 m; (c) Burial depth: 600 m.

From Figure 2, it is obvious that the resolution of the marine CSEM method becomes poor with the increasing of the depth of the anomalous body. According to Mittet and Morten [28], we have established a program that can calculate the sensitivity of each receiver relative to the transmitter and draw the results of the sensitivity of all receivers to different transmitters. Here, we chose 3% for the value of α [28].

Since the horizontal extent and vertical depth of the abnormal bodies of our seven models are the same, we decide to select the abnormal body in Figure 1 with a resistivity of $102 \Omega \cdot m$ for the sensitivity analysis. It is obvious from Figure 3 that the sensitivity curves all show two clear peaks which correspond to the extent of the abnormal body. In the signal transmitted by the transmitter and received by the receiver, there is a targets' influence on the sensitivity within a location range of ~ 5 km, which will offset the effect, so there will be double peaks, due to the difference between the two sides of the receivers.

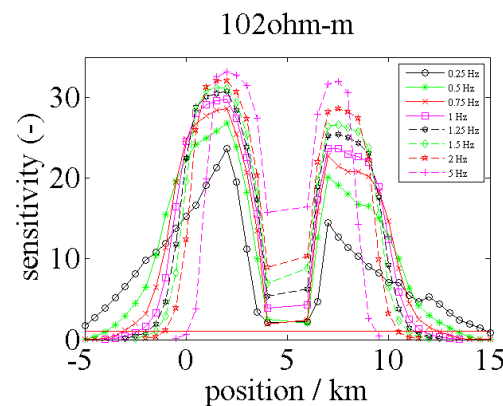


Figure 3. The sensitivity to target model at the receiver's location.

In order to explore the effects of frequency on the sensitivity of the marine CSEM method, we select the same model (i.e., the one used above) and select the sensitivity of the receiver at 2000 and 7000 m. The test results are shown in Figure 4. Clearly, we see that the sensitivity of the marine CSEM method shows a sharp increase at lower frequencies (< 2 Hz), independent of the receiver's depths. Then the sensitivity increases very gently when the frequency is above 2 Hz. Therefore, the natural gas hydrate deposit can be detected by marine CSEM method with high sensitivity in high frequency.

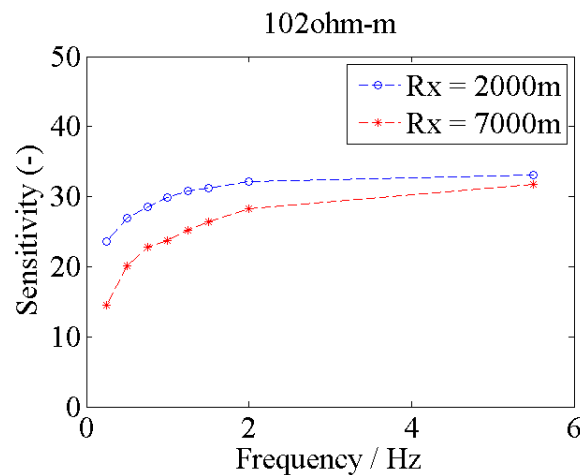


Figure 4. CSEM sensitivity study result related to frequency.

At last, we test the sensitivity of different resistivity models with the fixed frequency (2 Hz) and receiver location ($R_x = 2000$ m) (Figure 5). We set the resistivity of the models to be 102, 52, 22, 12, 10, 6, 5 and 4 $\Omega \cdot m$, respectively. From Figure 5 above we see clearly that the sensitivity drops with the decrease of the resistivity of the abnormal body, implying that it is difficult to detect the low resistivity natural gas hydrate. For the gas hydrate deposit exploration, high frequency CSEM method is required.

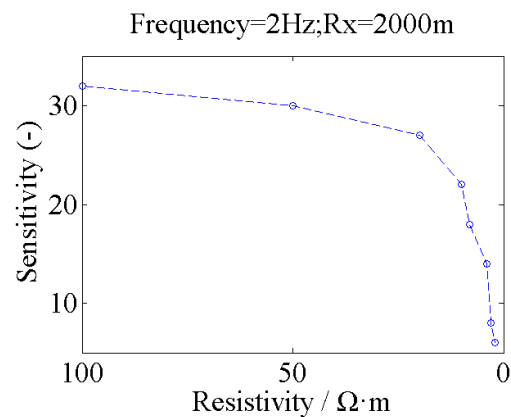


Figure 5. CSEM sensitivity varies with targets resistivity.

4. Discussion and Conclusions

In this paper, we explored the resolution and sensitivity of the marine CSEM method, where the lateral resistance of anomalous objects will affect the resolution. We explored the lowest detectable ATR of the CSEM method model through different resistivity models, and obtained the influence of different ATR on the model resolution. We find that when $ATR = 500$, the resolution of the abnormal body is relatively poor. Therefore, we conclude that the minimum ATR that makes the model resolution valuable is 600. That is, we can still get a good resolution when the product of the resistivity difference between the anomalous body and the surrounding seawater and the thickness of the model is no less than 600. This conclusion can enable us to reduce a lot of false anomaly judgments in the case of specific natural gas hydrate exploration and also reduce unnecessary workload. For example, when the thickness of the abnormal body is determined, we can determine the minimum resistivity that can be detected, and when the resistivity of the gas hydrate is roughly determined, we can estimate at least the thickness of the gas hydrate to be detected. In the mean time, we used one of the figures to explore its sensitivity, and we found that we can determine the location of abnormal bodies through sensitivity. This saves time and cost. With traditional methods, we need multi-step inversions to determine the lateral

extent of the anomaly, which requires a lot of time and money. However, the sensitivity investigation in this article can enable us to determine the horizontal occurrence range of natural hydrate without performing inversion, thereby reducing the drilling failure rate in gas hydrate detection and greatly saving exploration costs for natural gas hydrates. At the same time, we found that under the same conditions, high-frequency marine CSEM method detection has higher sensitivity than low-frequency detection. Therefore, we can obtain higher sensitivity by increasing the detection frequency. And higher resistivity corresponds to higher sensitivity, which is also in line with our perception.

Author Contributions: Conceptualization, Z.G. and Y.Y.; methodology, Z.G.; software, Y.Y., M.J.; validation, J.L., Y.Y. and B.W.; formal analysis, X.W.; investigation, X.W.; resources, Z.G.; data curation, Z.G.; writing—original draft preparation, Z.G., Y.Y.; writing—review and editing, Z.G., B.W.; visualization, X.W.; supervision, J.L.; project administration, J.L.; funding acquisition, Z.G. All authors have read and agreed to the published version of the manuscript.

Funding: This research was funded by National Natural Science Foundation of China (42074169; 41804073). It is funded by Investigating Project of China Geological Survey–Natural gas hydrate database update and service (DD20190216). Project is supported by the Fundamental Research Funds for the Central Universities of Central South University (2021zzts0802;CX20210289;2021zzts0828). Project also supported by National Training Program of Innovation and Entrepreneurship for Undergraduates (2021105330060).

Data Availability Statement: The datasets are available. The research who wants to use my synthetic data can order it from the first author by email guozhenwei@csu.edu.cn.

Acknowledgments: We would like to thank Kerry Key to share the MARE2DEM for us to finish this research.

Conflicts of Interest: The authors declare no conflict of interest.

References

1. Kvenvolden, K.A. Gas hydrates—Geological perspective and global change. *Rev. Geophys.* **1993**, *31*, 173–187. [[CrossRef](#)]
2. Milkov, A.V.; Sassen, R. Economic geology of offshore gas hydrate accumulations and provinces. *Marine Petr. Geol.* **2002**, *19*, 1–11. [[CrossRef](#)]
3. Sloan, E.D., Jr.; Koh, C.A. *Clathrate Hydrates of Natural Gases*; CRC Press: Boca Raton, FL, USA, 2007.
4. Dawe, R.A.; Thomas, S. A large potential methane source—Natural gas hydrates. *Energy Sour. Part A* **2007**, *29*, 217–229. [[CrossRef](#)]
5. Eidesmo, T.; Ellingsrud, S.; MacGregor, L.M.; Constable, S.; Sinha, M.C.; Johansen, S.E.; Kong, F.N.; Westerdah, H. Sea Bed Logging (SBL), a new method for remote and direct identification of hydrocarbon filled layers in deep-water areas. *First Break* **2002**, *20*, 144–152. [[CrossRef](#)]
6. Johansen, S.E.; Amundsen, H.E.F.; Røsten, T.; Ellingsrud, S.; Eidesmo, T.; Bhuiyan, A.H. Subsurface hydrocarbons detected by electromagnetic sounding. *First Break* **2005**, *23*, 1–36. [[CrossRef](#)]
7. Constable, S.; Weiss, C.J. Mapping thin resistors and hydrocarbons with marine EM methods: Insights from 1D modeling. *Geophysics* **2006**, *71*, G43–G51. [[CrossRef](#)]
8. Constable, S.; Srnka, L.J. An introduction to marine controlled source electromagnetic methods for hydrocarbon exploration. *Geophysics* **2007**, *72*, WA3–WA12. [[CrossRef](#)]
9. Evans, R.L.; Sinha, M.C.; Constable, S.C.; Unsworth, M.J. On the electrical nature of the axial melt zone at 13° N on the East Pacific Rise. *J. Geophys. Res. Solid Earth* **1994**, *99*, 577–588. [[CrossRef](#)]
10. Macgregor, L.M.; Constable, S.; Sinha, M.C. The Ramesses experiment -III. Controlled source electromagnetic sounding of the Reykjanes Ridge at 57°45' N. *Geophys. J. Int.* **1998**, *135*, 772–789. [[CrossRef](#)]
11. Edwards, R.N. On the resource evaluation of marine gas hydrate deposits using sea -floor transient electric dipole-dipole methods. *Geophysics* **1997**, *62*, 63–74. [[CrossRef](#)]
12. Marina, G.P.; Yuri, G.S.; Petr, A.D.; Denis, V.V.; Yulia, I.K. Electromagnetic field analysis in the marine CSEM detection of homogeneous and inhomogeneous hydrocarbon 3D reservoirs. *J. Appl. Geophys.* **2015**, *119*, 147–155. [[CrossRef](#)]
13. Streich, R. Controlled-source electromagnetic approaches for hydrocarbon exploration and monitoring on land. *Surv. Geophys.* **2016**, *37*, 47–80. [[CrossRef](#)]
14. Schwalenberg, K.; Engels, M.; Rippe, D.; Scholl, C. Marine CSEM for Gas Hydrate Exploration Using a Seafloor-towed Multi-receiver System. In Proceedings of the 76th EAGE Conference and Exhibition-Workshops, Amsterdam, The Netherlands, 16–19 June 2014; p. cp-401-00067. [[CrossRef](#)]
15. Schwalenberg, K.; Rippe, D.; Koch, S.; Scholl, C. Marine-controlled source electromagnetic study of methane seeps and gas hydrates at Opouawe Bank, Hikurangi Margin, New Zealand. *J. Geophys. Res. Solid Earth* **2017**, *122*, 3334–3350. [[CrossRef](#)]

16. Chen, K.; Jing, J.E.; Zhao, Q.X.; Luo, X.H.; Tu, G.H.; Wang, M. Ocean bottom EM receiver and application for gas-hydrate detection. *Chin. J. Geophys.* **2017**, *60*, 4262–4272. (In Chinese)
17. Tharimela, R.; Augustin, A.; Ketzer, M.; Cupertino, J.; Miller, D.; Viana, A.; Senger, K. 3D controlled-source electromagnetic imaging of gas hydrates: Insights from the Pelotas Basin offshore Brazil. *Interpretation* **2019**, *7*, SH111–SH131. [[CrossRef](#)]
18. Weitemeyer, K.A. *Marine Electromagnetic Methods for Gas Hydrate Characterization*; University of California: San Diego, CA, USA, 2008.
19. Edwards, R.N.; Nobes, D.C.; Gomez-Trevino, E. Offshore electrical exploration of sedimentary basins: The effects of anisotropy in horizontally isotropic, layered media. *Geophysics* **1984**, *49*, 566–576. [[CrossRef](#)]
20. Rodi, W.L. A technique for improving the accuracy of finite element solutions for MT data. *Geophys. J. Int.* **1976**, *44*, 483–506. [[CrossRef](#)]
21. Jupp, D.L.B.; Vozoff, K. Two-dimensional magnetotelluric inversion. *Geophys. J. Int.* **1977**, *50*, 333–352. [[CrossRef](#)]
22. Farquharson, C.G.; Oldenburg, D.W. Approximate sensitivities for the electromagnetic inverse problem. *Geophys. J. Int.* **1996**, *126*, 235–252. [[CrossRef](#)]
23. McGillivray, P.R.; Oldenburg, D.W. Methods for calculating Fréchet derivatives and sensitivities for the non-linear inverse problem: A comparative study. *Geophys. Prospect* **1990**, *38*, 499–524. [[CrossRef](#)]
24. McGillivray, P.R.; Oldenburg, D.W.; Ellis, R.G.; Habashy, T.M. Calculation of sensitivities for the frequency-domain electromagnetic problem. *Geophys. J. Int.* **1994**, *116*, 1–4. [[CrossRef](#)]
25. Spies, B.R.; Habashy, T.M. Sensitivity analysis of crosswell electromagnetics. *Geophysics* **1995**, *60*, 834–845. [[CrossRef](#)]
26. Gribenko, A.; Zhdanov, M. Rigorous 3D inversion of marine CSEM data based on the integral equation method. *Geophysics* **2007**, *72*, 540–552. [[CrossRef](#)]
27. Kaputerko, A.; Gribenko, A.; Zhdanov, M. Sensitivity analysis of Marine CSEM surveys. In *SEG Technical Program Expanded Abstracts*; Society of Exploration Geophysicists (SEG): Houston, TX, USA, 2007; pp. 609–613. [[CrossRef](#)]
28. Mittet, R.; Morten, J.P. The marine controlled-source electromagnetic method in shallow water. *Geophysics* **2013**, *78*, E67–E77. [[CrossRef](#)]
29. Scholl, C.; Edwards, R.N. Marine downhole to seafloor dipole-dipole electromagnetic methods and the resolution of resistive targets. *Geophysics* **2007**, *72*, WA39–WA49. [[CrossRef](#)]
30. Gao, G.; Alumbaugh, D.; Chen, J.; Eyl, K. Resolution and uncertainty analysis for marine CSEM and crosswell EM imaging. In *SEG Technical Program Expanded Abstracts*; Society of Exploration Geophysicists (SEG): Houston, TX, USA, 2007; Volume 27, pp. 623–627. [[CrossRef](#)]
31. Morten, J.P.; Bjørke, A.K.; Nguyen, A.K. Hydrocarbon reservoir thickness resolution in 3D CSEM anisotropic inversion. In *SEG Technical Program Expanded Abstracts 2010*; Society of Exploration Geophysicists: Tulsa, OK, USA, 2010; pp. 599–603. [[CrossRef](#)]
32. Brown, V.; Hoversten, M.; Key, K.; Chen, J. Resolution of reservoir scale electrical anisotropy from marine CSEM data. *Geophysics* **2011**, *77*, 147. [[CrossRef](#)]
33. Moghadas, D.; Engels, M.; Gehrman, R.A.S.; Schwalenberg, K. 3D numerical modelling and 1D inversion and resolution analysis of time-domain marine controlled source electromagnetic data. In *Proceedings of the Schmucker Weidelt Kolloquium, Elektromagnetische Tiefenforschung, Kirchhundem-Rahrbach, Germany, 23–27 September 2013*; pp. 104–108.
34. Sasaki, Y. Resolution of shallow and deep marine CSEM data inferred from anisotropic 3D inversion. In *SEG Technical Program Expanded Abstracts*; Society of Exploration Geophysicists (SEG): Houston, TX, USA, 2013. [[CrossRef](#)]
35. Blatter, D.; Key, K.; Ray, A.; Gustafson, C. Bayesian Joint Inversion of Surface-Towed CSEM and MT Data: Quantifying the Resolution Gain. In *Proceedings of the 24th EM induction Workshop, Helsingør, Denmark, 12–19 August 2018*.
36. Ren, Z.; Kalscheuer, T. Uncertainty and resolution analysis of 2D and 3D inversion models computed from geophysical electromagnetic data. *Surv. Geophys.* **2020**, *41*, 47–112. [[CrossRef](#)]
37. Lee, M.W.; Collett, T.S. Scale-dependent gas hydrate saturation estimates in sand reservoirs in the Ulleung Basin, East Sea of Korea. *Marine Petr. Geol.* **2013**, *47*, 195–203. [[CrossRef](#)]
38. Key, K. MARE2DEM: A 2-D inversion code for controlled-source electromagnetic and magnetotelluric data. *Geophys. J. Int.* **2016**, *207*, 571–588. [[CrossRef](#)]
39. Matsumoto, R.; Takedomi, Y.; Wassada, H. Exploration of marine gas hydrates in Nankai Trough, offshore Central Japan. In *Proceedings of the AAPG Annual Convention, Denver, CO, USA, 3–6 June 2001*; Volume 36.